

Tribometrological Studies In Bioengineering

Dr. Norm Gitis, Center for Tribology, Inc.
1715 Dell Ave., Campbell, CA 95008, www.cetr.com

ABSTRACT

A novel experimental technology for studies of biological and bioengineered materials and structures has been developed. It is based on precision servo-control of forces or displacements and simultaneous real-time multi-sensor monitoring of deformations, forces and torques in all directions, contact acoustic emission, contact or surface electrical resistance or impedance, temperature, and digital microscopy, optionally accompanied with periodic atomic force microscopy of the test surfaces. Examples of the implementation of this technology in the Biomechanical Micro-tester mod. UMT are described for such diverse biotech applications as studies of prosthetic devices, skin, hydrogels, beauty care products, shaving blades and creams, toothpastes and dental materials, surgical sutures and needles, balloons and stent grafts, bio-fluids and bio-tissues.

Introduction

Biological and bioengineered materials and coatings present a wide spectrum of durability challenges. Over 200 bones and 600 muscles in the human body can fail due to numerous reasons. The biological lubricants produced by the body, including saliva, tears and synovial fluid, can dry up or deteriorate because of different effects. Artificial hips, knees, elbows and fingers cannot yet fully mimic the functional and tribological performance of the biological joints. Artificial heart valves, blood pumps and kidneys require much testing and improvement. Ocular tribology deals with friction in contact lenses and eyelids, lubricated with tears and complicated by eye blinking. Durability of artificial teeth from porcelain, gold and acrylic has to be increased to the level of tooth enamel. Surgical needles and shaving blades have to maintain their sharpness so their cutting force stays low. Surgical sutures and cosmetic products should maintain low friction, balloons and stent grafts require good durability and flexibility.

All these diverse tasks require much testing and understanding. The traditional engineering problems of correlating benchtop material test results with the real-life performance of components from the same materials are even more important in bioengineering, where full and comprehensive simulation of the in-vivo conditions is often impossible. The scientists need better test equipment, instrumentation and procedures to mimic the human body more accurately. To meet this demand, this paper describes a multi-sensing technology, realized in a tester of modular design, which seems to provide the most useful test platform for the successful solution of the above challenges.

State-of-the Art Tribo-Metrology

The multi-sensing technology, which includes simultaneous real-time monitoring of deformations, forces and torques in all directions, contact acoustic emission, contact or surface electrical resistance or impedance, temperature, and digital microscopy, optionally accompanied with periodic atomic force microscopy of the test surfaces, allows for the most comprehensive evaluation of materials and components. The more signals are monitored, the better off we are in our process and materials control and optimization. These multi-sensor measurements have been implemented on a commercially available Bio-Mechanical Tester mod. UMT, a photo of which is shown in Fig. 1. It provides comprehensive tribological measurements for various types of samples in a variety of biomedical applications. For example, it is successfully utilized for testing bathroom tissues on skin, soap on skin, surgical staples and sutures, medical needles, shaving blades, after-shave lotions, tooth pastes and tooth brushes, stent grafts and balloons.

The UMT is capable of providing precision linear and rotational, including reciprocation, motions with programmable speeds and accelerations in the range from 0.1 $\mu\text{m/s}$ to 10 m/s (8 orders of magnitude) and programmable positions (displacements) in the range from 0.5 μm to 150 mm (over 5 orders of magnitude). A normal load is controlled via a closed-loop servomechanism with user-defined tolerances, and can be programmed to be either constant or changing gradually or by steps in the range from 10 μN to 1 kN (8 orders of magnitude). A number of parameters, including forces and displacements in all X, Y and Z directions, electrical contact or surface resistance, capacitance or impedance, deformation (elastic, plastic, creep) or wear depth, temperature, and contact acoustic emission can all be measured and recorded simultaneously, with a sampling rate of 20 kHz. Also, digital video with optical microscopy and scanning force microscopy are readily available.



Figure 1. Biomechanical Universal Micro Tester Mod. UMT

Dermatological Studies

Skin health and beauty is a concern for people of all ages. Physiologically, skin is the first line of defense against any environment, and it is repeatedly subjected to physical and chemical damage. Over the course of time a person's skin undergoes changes, and to maintain skin health, it is important to quantitatively follow these changes. Sometimes these skin changes are visible, such as wrinkles, blemishes or rashes. In other cases, the changes may not be easily discernable without a quantitative assessment of skin properties. Some skin care products inhibit water evaporation from the skin, some compounds absorb and release hydrating elements into the skin, other compounds provide a greasy texture, while others elicit a more sticky texture. Quantification of these properties is crucial in the development of new skin care products.

The bulk of dermatological observations are based on qualitative visual or papillary data. The unique multi-sensing technology described in this paper fills the void in the fields of dermato-physiology, dermato-pharmacology, dermato-toxicology and cosmetology. Utilization of the multi-sensing technology with real-time high frequency data acquisition provides a fast and quantitative assessment of skin dryness and moisturization, early diagnosis of skin diseases or of the deterioration in skin functions at a stage that may not be easily discernable visibly, development of skin cosmetics and medicine.

The UMT has been utilized for both *in-vitro* testing on the artificial or cut-off skin (laid on the sample table seen in Fig. 1) and *in-vivo* testing on people's arms (see photo in Fig. 2), fingers (see photo in Fig. 3) and other body parts (not shown). The measurement probe, a 12-mm copper/Teflon cylinder attached to a proprietary suspension system (though in some tests Teflon and stainless steel balls were used), was pressed onto the skin with a load of 0.1 N, sufficient to maintain a contact with the skin, but not too high to avoid skin macro-deformations and focus the measurements on the skin surface only. For studies involving under-skin layers and tissues, higher loads up to 5 N were used. The probe was moved across the skin at the speed of 1 mm/s for 10 mm (though some tests were performed at higher speeds of 5 cm/s on longer traces, to better simulate the motion of a person's finger when checking her or his skin, which may be important for characterization and marketing of cosmetic products). During probe sliding, the dynamic friction coefficient was measured with a proprietary strain-gauge sensor, monitoring simultaneously and independently both normal load and friction force, with the resolution of 0.1 mN; also, a friction variation coefficient was calculated as its amplitude-to-mean ratio: as the friction variation coefficient increases, the skin is expected to be stickier or rougher. In-situ electrical measurements were performed by applying an alternating current of a small amplitude 10 μ Amps, with frequency of 10 kHz, measuring the voltage and calculating the electrical impedance.

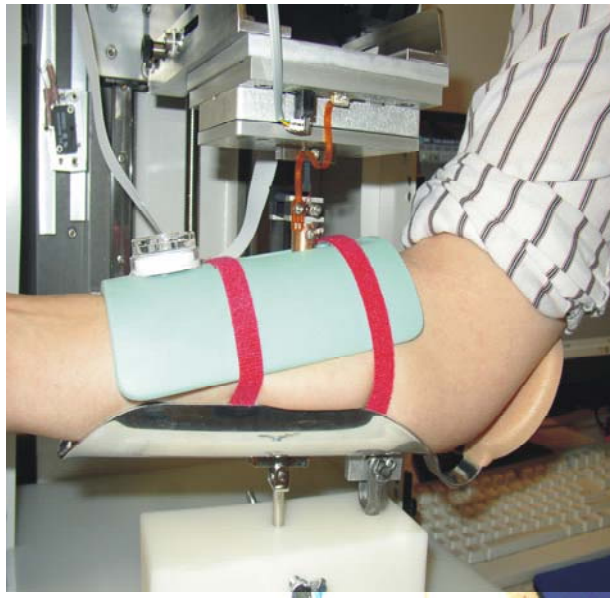


Figure 2. Forearm In-Vivo Measurements



Figure 3. Finger In-Vivo Measurements

Sixty healthy adult volunteers were tested, classified to a certain race and age group. The tests were carried out in a controlled room with constant temperature and humidity. Volunteers were asked to refrain from wearing creams prior to coming to the test. The test sites on their arms were cleaned with isopropyl alcohol prior to testing. The tests were conducted on the right and left volar forearms. Different treatments were administered, including no treatment, occlusion by wrapping the arm in polyvinylidene chloride or PVDC (saran wrap) for 30 min to prevent water loss, glycerin applied at 3 mg/cm², and petrolatum applied at 0.5 mg/cm² (interchanged between the sites). Measurements of the petrolatum and glycerin treated arms were taken after leaving the treatments on for 1 min and dabbing the skin with a paper towel to remove excess.

No significant differences were found in either friction or electrical parameters of volar forearms between age, gender, or ethnicity. The untreated skin on the volar forearm produced similar frictional and electrical characteristics across gender, age, and ethnicity. Since there is some variation with anatomical site on the volar forearm, comparisons among chemicals on the same volunteer can be done by comparing similar anatomical sites on the right and left volar forearm. The similarity between young and old volar forearm skins is due to the volar forearm being protected from the sun. Thus, the volar forearm may be a good anatomical site for testing skin care products.

All of the skin treatments showed no significant differences between gender, age and ethnicity, but quite dramatic differences as a result of the different interventions. Occluded skin showed an increase in friction and a decrease in impedance (Fig-s 4 and 5). As the PVDC covered the skin, it prevented the water evaporation, so the trapped water decreased the impedance.

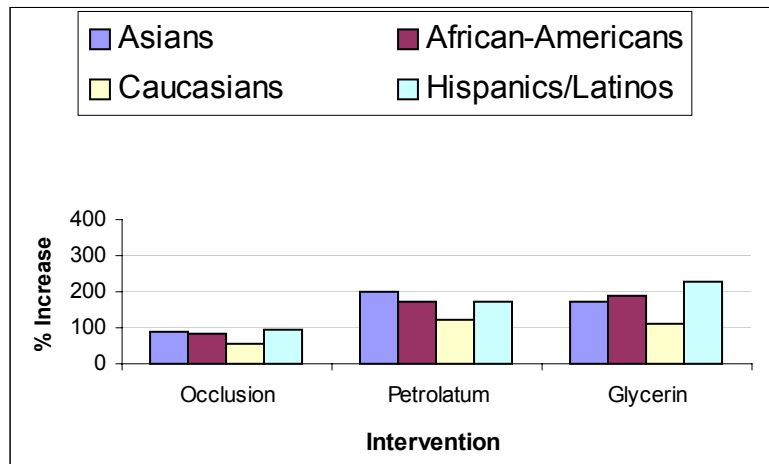


Figure 4. Increase in Friction For Three Skin Treatments

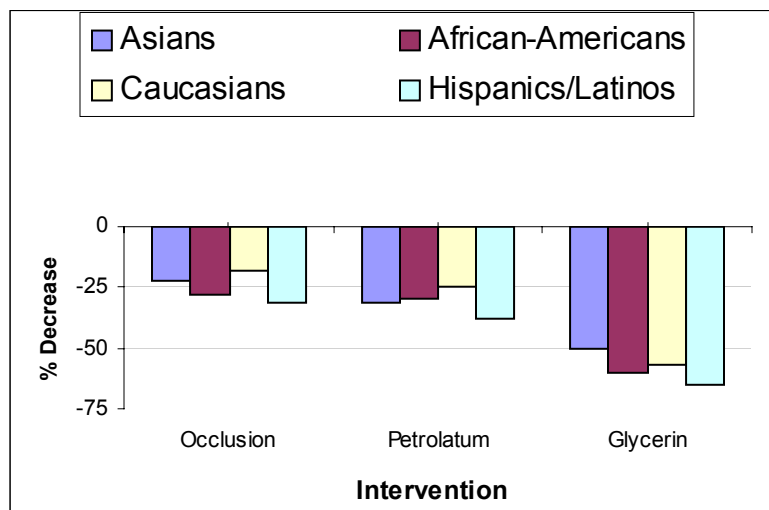


Figure 5. Decrease in Impedance for Three Skin Treatments

The increased hydration made the skin stickier due to water-mediated adhesion between the probe and the skin, which resulted in the increased both friction and friction variation coefficient for the occluded skin (Fig-s 4 and 6). Petrolatum served as a barrier for the water loss and so increased skin hydration, which lowered the skin impedance by a similar amount as the occlusion (Fig. 5). Friction for the petrolatum-treated skin, however, was higher than after the PVDC occlusion (Fig. 4), indicating that the petrolatum may have been absorbed into the skin, unlike the PVDC. The friction variation coefficient indicated that the petrolatum lowered the skin stickiness (Fig. 6). These results give a solid quantitative support for the qualitative perception that petrolatum is greasy and tends to make skin more slippery. Glycerin increased friction similarly to that of petrolatum; however, it dropped impedance to a much greater degree than either petrolatum or PVDC occlusion did. This may be reflective of the higher rate and amount of glycerin absorbed directly into the skin, which may allow for higher skin hydration, as measured by the lower skin impedance. The highest friction variation coefficient showed that glycerin increased the skin stickiness the most (Fig. 6).

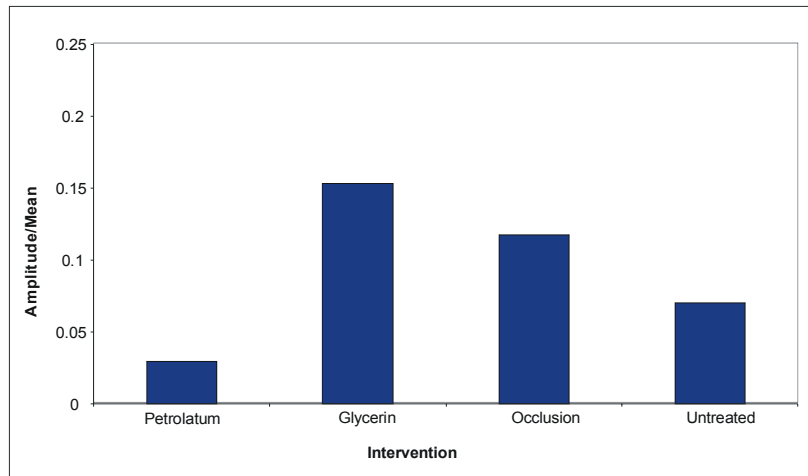


Figure 6. Amplitude-to-Mean Ratio for Three Skin Treatments

Hydration is a complex phenomena influenced by intrinsic (i.e. age, anatomical site) and extrinsic (i.e. ambient humidity, chemical exposure) factors. In general, a skin response to water is quite complex, as the very wet skin also has low friction due to the hydrodynamic effects, while the very dry (clinically dry) skin is rough and increases a mechanical component of friction. We performed an experimental comparison of three different moisturizing creams: an inexpensive one, a moderately priced daytime cream, and an expensive nighttime cream. Ten healthy adult volunteers were tested on the same locations of both their right and left volar forearms. Each test included three sequential unidirectional runs, done before cream application (to establish the reference levels of the test parameters), then every 5 minutes for 1 hour, then after 5 hours, finally next day after 24 hours. The frictional and electrical data were very consistent between all the volunteers. All three moisturizers had the same qualitative effect of increasing friction and decreasing electrical impedance, but quantitatively differed substantially. The inexpensive cream lasted for less than an hour, the medium-quality cream lasted for several hours, the effect of the most-expensive cream was still measurable a day later. These tests provide a scientific justification to the pricing of these creams, as they quantify their functional quality.

Hip Replacement Studies

Artificial hips have been one of the most successful orthopedic devices, and are implanted in quantities of hundreds of thousands annually. Still, they last less than 15 years and have to be replaced via another major surgery. The cobalt-chromium or alumina head wears a socket made from either ultra-high molecular weight cross-linked polyethylene or ceramics, even in the presence of a synovial fluid.



Figure 7. Hip Joint Test Setup

We performed hip-simulating tests with in-situ monitoring tribological parameters of the metal head - polymer cup hip joint with bovine serum. The UMT can easily perform a combination of several simultaneous motions of both upper and lower specimens; the setup shown in Figure 7. The metal head was mounted on a tapered shaft with a flat plate, attached to a force/torque sensor (for simultaneous normal load and friction torque measurements) on a tilting and reciprocating drive, the polymer cup was mounted in a fluid container on a rotational drive. A small proprietary acoustic emission sensor was attached to the flat plate on the side opposite to the shaft with the head. The samples were fully immersed in a bovine serum. An applied vertical load was cycled from 0.3 to 1 kN, using a closed-loop feedback servo-control. To accelerate wear processes, the test was performed in a start-stop mode, with the drives cyclically accelerating, spinning for 30 sec, and decelerating to a full stop, while the bovine serum was not replenished and allowed to dry out, thus accelerating particle formation and accumulation.

During the tests, a normal force (F_z), friction torque (T_z), and AE signal were continuously monitored (since the polymer cup is non-conductive, contact electrical resistance was not monitored). During each start, the friction torque increased almost instantly and reached its maximum value corresponding to the full static friction (stiction). Then during the spin, the friction torque reduced, and when the drives stopped, friction torque dropped down almost to zero. In the beginning of the test, when the wear was insignificant, the AE signal remained at its near-zero level. The average values of T_z and AE from each cycle are plotted versus test time in Figure 8. The friction torque T_z grew within the first few hours due to run-in processes, then more or less stabilized for several hours while AE signal remained low. After some time, friction started to increase, while acoustics remained low, indicating a low level of mechanical interactions. Soon thereafter, the friction torque increased sharply and reached its maximum value, the AE signal showed occasional peaks and then increased its level dramatically (30 times higher than the initial level), reflecting a failure. The post-test sample observation showed that the bovine serum dried out and left a lot of residual particles, which caused the increases in both friction and acoustics. After fresh fluid was added into the cup, and the test continued, both friction and acoustics reduced comparing to their levels at the end of the first test, however, staying higher and less-stable than their pre-failure levels in the first test.

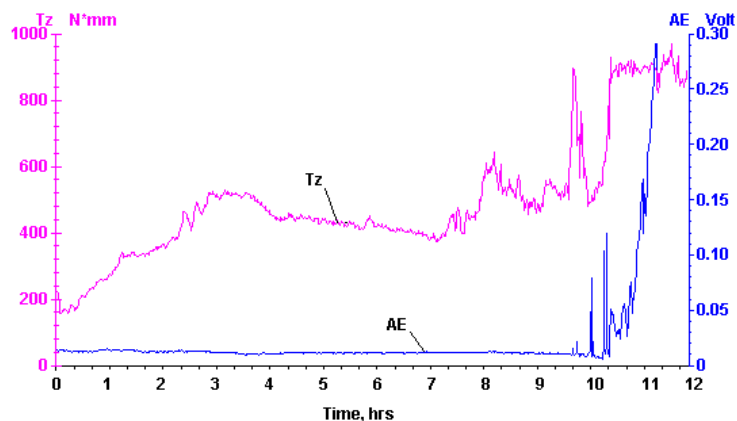


Figure 8. Friction Torque and AE Changes During Hip Replacement Accelerated Test

The above confirms that both tribological parameters of friction and acoustic emission are sensitive to the surface wear processes and can be used for in-situ wear monitoring during orthopedic life simulating tests. The friction torque seemed to show slightly higher sensitivity to wear during the break-in and pre-failure modes, the acoustic signal seemed to show slightly higher sensitivity to the presence of particles.

Testing of Tribological Properties of Contact Lenses

Hydrogel contact lenses have to have low static friction to ensure easy replacement, but sufficient friction to avoid slipping off. We tested several conventional and experimental lenses with curved surfaces of 14-mm diameter, with water content of 10-50%. The counter-samples were polished stainless steel and glass discs. The friction tests were performed on the setup shown in Figure 9. A contact lens was mounted in a holder with a stainless steel ball for a sample support, and attached to a dual-force sensor (for simultaneous normal load and friction force measurements) as the stationary upper specimen. The counter-disc was mounted on a rotational drive as the rotating lower specimen. A vertical load was maintained constant during the test, using a closed-loop feedback servo-control. Each lens was immersed in its packing solution, applied onto the disc surface; after each test the disc was cleaned and wiped. The tests were done at the same speed of 15 cm/s and three levels of load, 5 cN, 10 cN and 20 cN, for 30 s at each level.

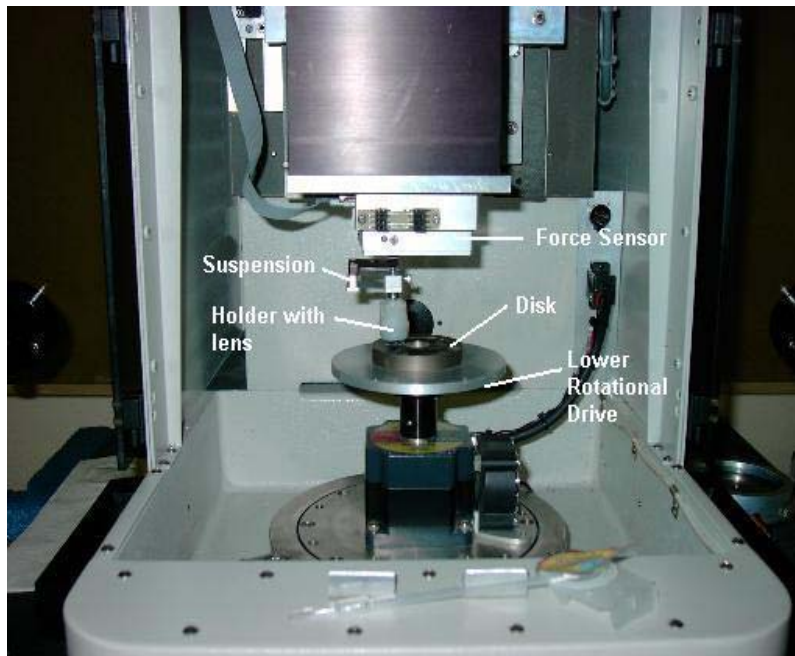


Figure 9. Friction Test Setup for Contact Lenses

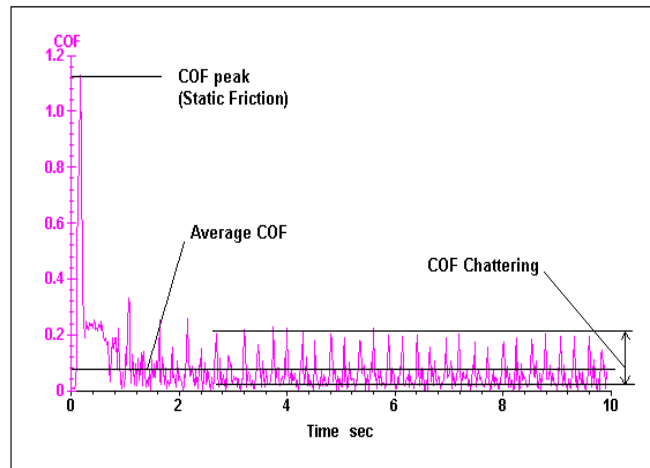


Figure 10. Friction Changes During Tests of Contact Lenses

During the tests, a coefficient of friction (COF) was continuously monitored. Its typical real-time graph is shown in Figure 10. In the beginning of the test, when the disc just starts to move, friction increases instantly and reaches the maximum value (COF Peak) called stiction, or full static friction. During the test, with the disc spinning at constant speed, friction drops and remains at a certain sliding level (COF Average). The friction standard deviation from the average level (COF Chatter) characterizes smoothness of the motion and presence or absence of stick-slip.

The graphs in Figures 11a to 11c show friction of seven types of contact lenses at three loads, on the glass disc. Focus contact lenses had overall the highest level of both sliding friction and friction chatter, but moderate static friction. Purevision lenses had higher average friction and friction chatter on steel, while lower friction and chatter on glass. Acuvue lenses had low friction at low load, but higher friction at higher loads. Biomedics lenses had low levels of sliding friction and friction chatter, but high static friction on steel. Proclear lenses also had low level of sliding friction and friction chatter, but high static friction.

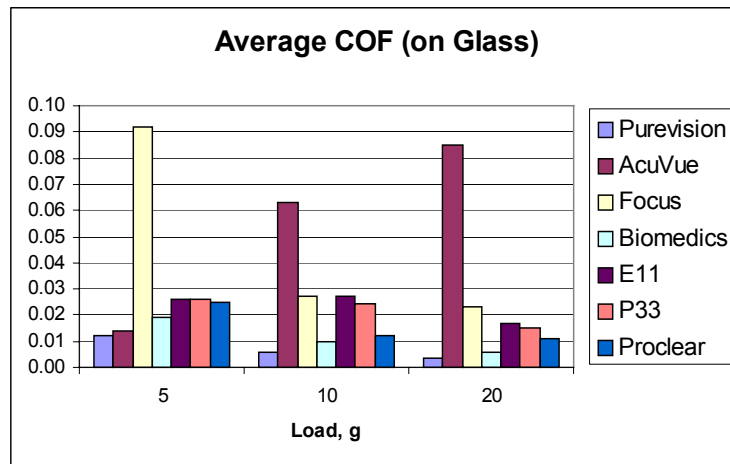


Figure 11a. Sliding Average Friction of Lenses On Glass

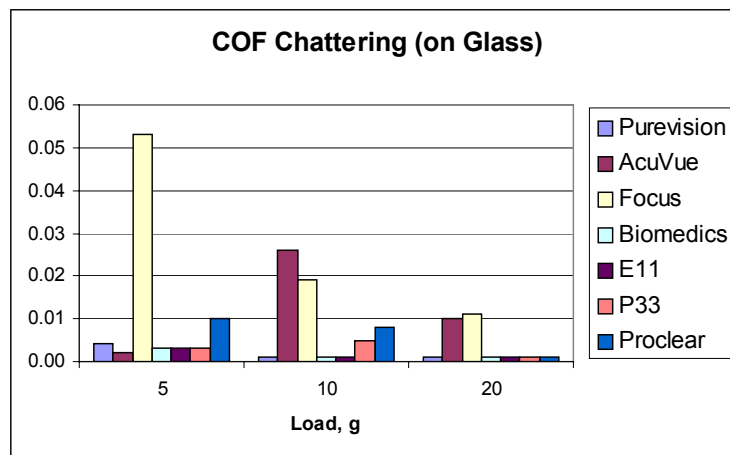


Figure 11b. Friction Chatter of Lenses on Glass

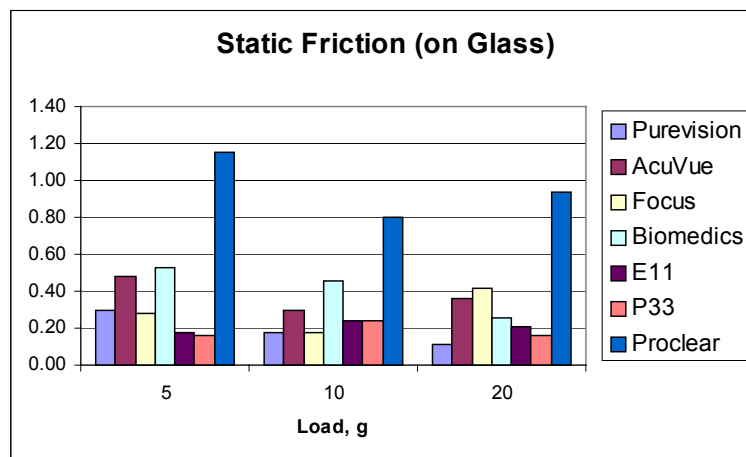


Figure 11c. Static Friction of Lenses on Glass

Testing of Surgical Needles

Two important functional parameters were measured for medical needles, the puncturing force into the skin, which may be related to the pain experienced by a patient and so has to be low, and the depth of needle penetration into the skin. The schematic of needle testing is shown in Figure 12. A needle was mounted on the upper holder and brought down, at the

constant speed, to punch into the artificial or cut-off skin, fixed on the lower table. Either the penetration depth is measured under a constant load, or the load is measured at a predetermined penetration depth. A close-loop feedback servo-control ensures either constant load or displacement. The needle is then pulled out for next penetration.

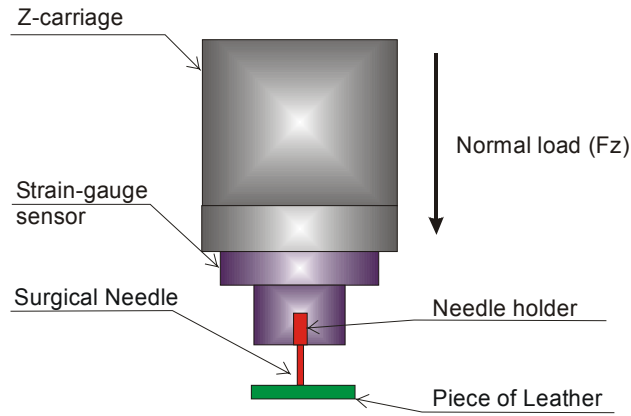


Figure 12. Setup for Needle Testing

At the constant load of 20 cN, we measured the change in penetration depth over 20 consecutive punctures. The plots of depth versus a number of punctures are shown in Figure 13. The depth decreased with a number of penetration times, indicating that the needles became dull. The Needle 1 had better sharpness durability than Needle 2 over time.

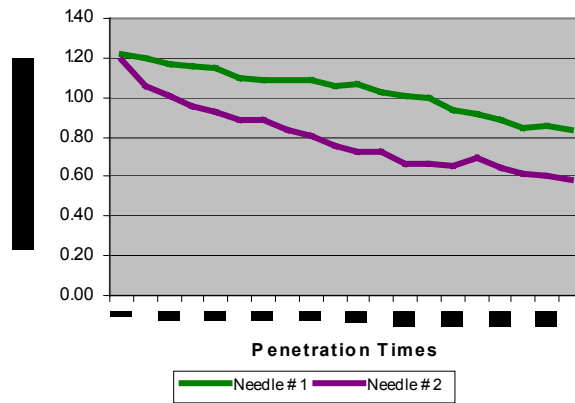


Figure 13. Needle Penetration Depth (mm) vs. Puncture Times

Tests of Surgical Sutures

Medical surgical sutures are tested for durability against either each other or a stainless steel rod. The schematic of suture testing is shown in Figure 14, where either the rod (left) or suture (right) mounted on the upper sample holder moves on the lower suture back and forth for a reciprocating length of 5 mm at a frequency of 1 Hz under a constant normal load of 5 cN. When the suture is worn to break, the normal force drops to zero, since there is no support for the abrasion. The time to abrade the suture to break is measured, based on monitoring friction force, normal force, and wear depth.

As shown in Figure 15, suture 1 exhibited better performance in both longer abrasion to failure and lower friction coefficient than suture 2.

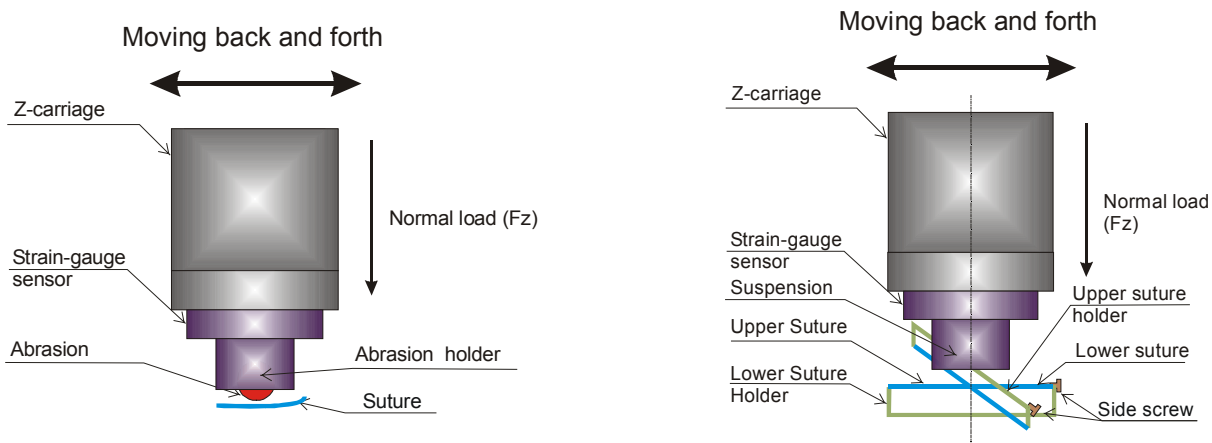


Figure 14. Setups for Rod-on-Suture (left) and Suture-on-Suture (right) Tests

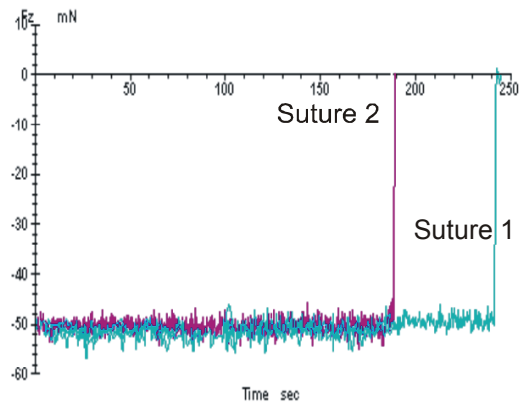


Figure 15. Normal load versus Abrasion Time

Balloon Flexibility

Medical balloons are tested for their elasticity. The schematic of balloon flexibility testing is shown in Figure 16. A balloon was mounted on the lower sample holder with three different methods: three point, cantilever, and flexible. A flat head screw was mounted on the upper holder and moved down to the surface of the balloon; this position was set as the zero position. Then, the displacement of screw was set to 0.5 mm and the screw was moved down and up twice several times at a speed of 0.05 mm/sec. Balloon A is more flexible than Balloon B, since for the same force, Balloon A exhibited a larger deflection.

Stent graft tests

Stent graft material (polyester woven cloth) was tested for durability. The schematic for graft material test is shown in Figure 17. A triangular piece of stent sheath was mounted on the upper sample holder and reciprocated over the graft material for a length of 5 mm at a frequency of 1.5 Hz under a constant normal load of 0.3 N. When the graft sample was worn through, the normal force and upper carriage position changed suddenly, since the support for the stent triangle also decreased suddenly. During a test, carriage position, friction force, normal force, time and coefficient of friction were recorded. The elapsed time for the graft material to wear through indicated abrasion resistance.

Conclusion

The described tests show how bio-materials can be evaluated for their tribological and mechanical properties, including abrasion and puncture resistance, elasticity, wear and friction, all with a single instrument. Other material properties, like fatigue, hardness and scratch resistance, can also be measured.

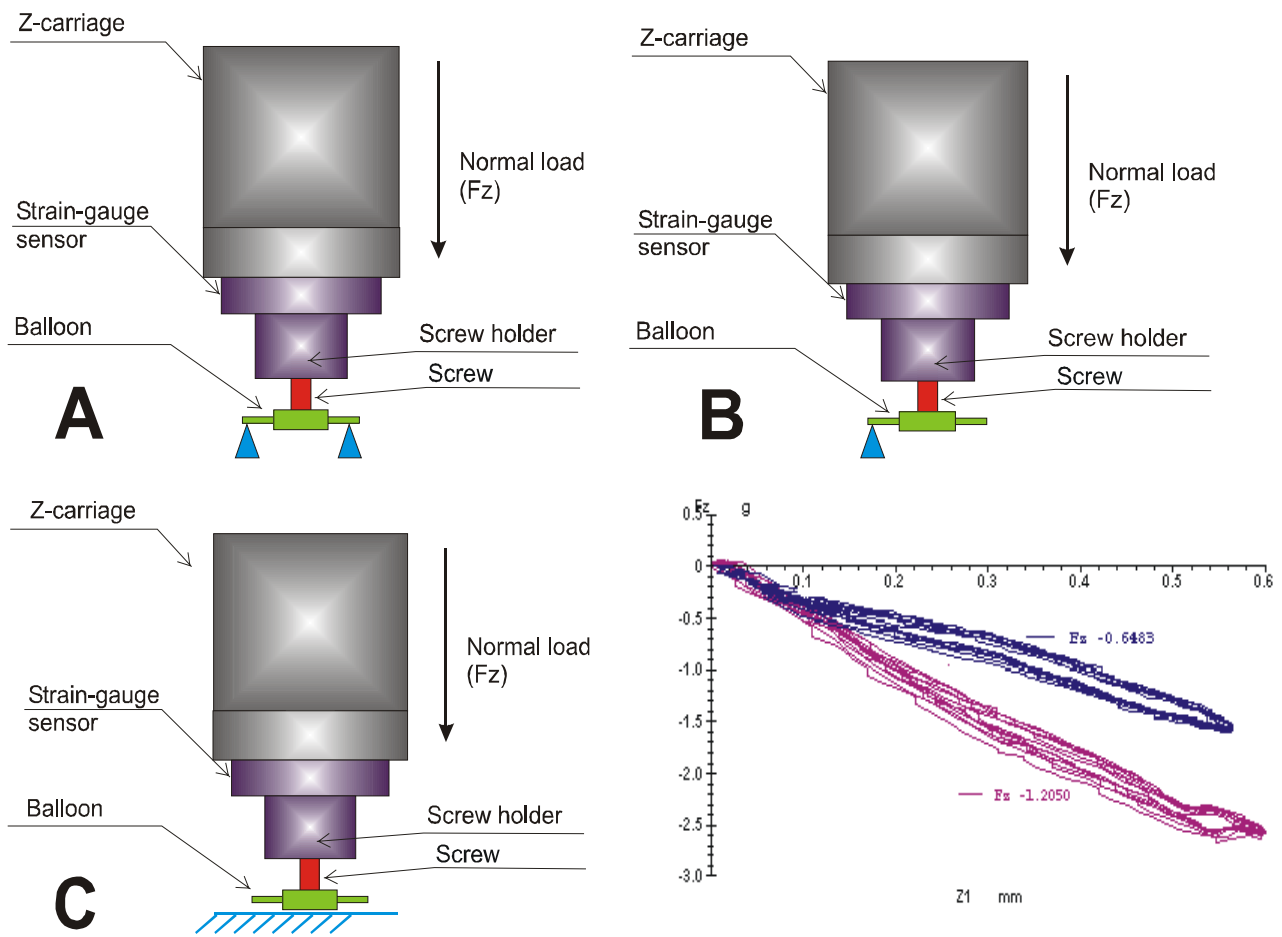


Figure16. Test Setup for balloon flexibility: A-three point; B-cantilever; C-flexible basis

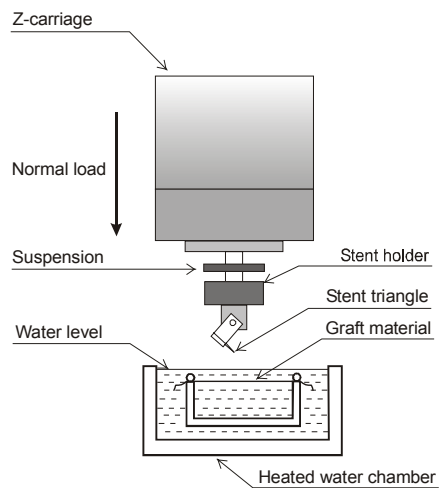


Figure 17. Setup for Stent Graft Testing